

IIIT HYDERABAD

[Robotics Research Center]



FINAL REPORT ON
AIRFOIL DESIGN ANALYSIS XFLR5
BACHELOR OF ENGINEERING
IN
INFORMATION TECHNOLOGY
(2022-2026)

BY
D. LEELA SHIVA KESHA RAO

Under the Guidance of

AVIJIT ASHE

(Teaching Assistant, IIIT Hyderabad)

VASAVI COLLEGE OF ENGINEERING
(AUTONOMOUS)



ACCREDITED BY NAAC WITH 'A++' GRADE

(Affiliated to Osmania University and Approved by AICTE)

Ibrahimbagh, Hyderabad-31

TABLE OF CONTENTS:

Abstract 1

Introduction..... 2

Objectives..... 3

Timeline & Resources..... 4

Geometry Import and Setup 5

Aerodynamic Simulations..... 12

Stall Behaviour Analysis..... 22

Performance Metrics 25

Comparative Study..... 27

Conclusion 30

References..... 31

ABSTRACT

This research investigates the aerodynamic performance of two distinct airfoil profiles, the NACA 4412 and NACA 0012, utilizing XFLR5 software to analyze their suitability for low-speed and high-speed aircraft applications, respectively. The study encompasses a comprehensive analysis of lift, drag, and moment coefficients, pressure distribution, and stall characteristics across varying angles of attack and Reynolds numbers. Through comparative analysis, the research aims to quantify the performance differences between the two airfoils, demonstrating the impact of airfoil geometry on aerodynamic behavior in different flight regimes. The findings highlight the NACA 4412's superior lift generation at low speeds and the NACA 0012's minimized drag at high speeds, validating their respective applications. This research provides valuable insights into airfoil selection and design considerations for aircraft operating under diverse flight conditions.

INTRODUCTION

Airfoil design is a critical aspect of aircraft engineering, directly influencing flight performance, efficiency, and stability. The selection of an appropriate airfoil is contingent upon the specific operational requirements of the aircraft, particularly its intended speed range. Different flight regimes demand specific airfoil characteristics. For instance, low-speed applications, such as those encountered during takeoff and landing, benefit from high-lift airfoils that enable operation at lower velocities. Conversely, high-speed aircraft, particularly those designed for transonic or supersonic flight, require airfoils that prioritize drag reduction to achieve optimal cruise efficiency.

This research focuses on the comparative analysis of two widely recognized airfoil profiles: the NACA 4412 and the NACA 0012. The NACA 4412, a cambered airfoil, is renowned for its superior lift generation capabilities at low speeds, making it a suitable choice for aircraft operating primarily at lower velocities. In contrast, the NACA 0012, a symmetrical airfoil, is designed to minimize drag at high speeds, making it ideal for aircraft intended for high-speed cruise and maneuvering. The analysis is conducted using XFLR5, a versatile and widely used software tool for airfoil analysis, enabling the evaluation of aerodynamic characteristics through computational simulations.

The primary objective of this study is to quantify and compare the aerodynamic performance of the NACA 4412 and NACA 0012 airfoils across a range of operational conditions, encompassing varying angles of attack and Reynolds numbers. By examining key aerodynamic parameters such as lift, drag, and moment coefficients, pressure distributions, and stall behavior, this research aims to provide a comprehensive understanding of the aerodynamic principles governing airfoil selection for diverse flight regimes. Ultimately, this research seeks to contribute to the understanding of airfoil behavior and provide valuable insights for aircraft designers and engineers in optimizing airfoil selection for specific flight conditions.

The methodological approach employed in this research combines theoretical analysis with computational fluid dynamics (CFD) simulations to generate comprehensive performance data. Special attention is given to the boundary layer behavior and flow separation characteristics that significantly impact airfoil performance near stall conditions. By systematically varying operational parameters and recording the resultant aerodynamic responses, this study establishes quantifiable performance metrics that enable direct comparison between the two airfoil profiles. Furthermore, the research examines the sensitivity of each airfoil to Reynolds number effects, providing insights into how scale factors influence performance across different aircraft sizes and flight velocities. These findings have relevance for aerospace engineers engaged in preliminary design phases, where airfoil selection represents a foundational decision with cascading effects throughout the aircraft development process.

AIRFOIL SELECTION AND ANALYSIS FOR LOW-SPEED AND HIGH-SPEED AIRCRAFT USING XFLR5

Objectives:

1. Evaluate and Quantify Aerodynamic Performance:

Scope: To systematically determine and quantify the aerodynamic characteristics of the selected airfoils (NACA 4412 and NACA 0012) across a range of operational conditions.

This involves generating precise data on lift, drag, and moment coefficients, which are fundamental to understanding an airfoil's performance. Additionally, the project will map pressure distributions across the airfoil surfaces to visualize and analyze the forces at play. Furthermore, lift-drag polars will be generated to comprehensively represent the airfoil's performance envelopes.

2. Analyze and Compare Airfoil Suitability for Specific Flight Regimes:

Scope: To assess and compare the performance of the airfoils in the context of their intended applications (low-speed vs. high-speed flight).

This requires a detailed examination of how each airfoil's aerodynamic characteristics align with the requirements of its respective flight regime. For instance, the NACA 4412's high-lift capabilities will be evaluated for low-speed applications, while the NACA 0012's low-drag properties will be assessed for high-speed scenarios.

3. Investigate Stall Behavior:

Scope: To accurately identify and analyze the stall characteristics of each airfoil, including the stall angle and the aerodynamic behavior during and after stall.

Stall is a critical phenomenon affecting aircraft safety and performance. This objective will involve precise determination of the angle of attack at which stall occurs for each airfoil. The research will also delve into the changes in lift and drag forces as the airfoil approaches and exceeds the stall angle, providing valuable insights into the airfoil's stability and control characteristics.

4. Provide a Comparative Analysis of Performance Metrics:

Scope: To generate and compare key performance metrics for both airfoils, enabling a quantitative assessment of their relative merits.

This involves calculating and comparing metrics such as the lift-to-drag ratio (L/D), zero-lift drag coefficient (C_{d0}), maximum lift coefficient ($C_{l_{max}}$), and moment coefficient (C_m). These metrics will provide a clear, data-driven comparison of the airfoils' aerodynamic efficiency and stability.

5. Document and Visualize Results:

Scope: To effectively document and visualize the research findings through clear, concise diagrams, graphs, and tables.

This ensures that the research outcomes are easily interpretable and accessible to a wider audience. Visualizations, such as pressure distribution plots and lift-drag polars, will play a crucial role in conveying the complex aerodynamic phenomena under investigation.

TIMELINE & RESOURCE ESTIMATION:

Objective	Timeline (Approx)	Resources	Adjustments
Evaluate and Quantify Aerodynamic Performance	1 week	XFLR5 software, computational resources, airfoil coordinate data	Focus on key angles of attack; streamline pressure distribution plots.
Analyze and Compare Airfoil Suitability for Specific Flight Regimes	1 week	Data from Objective 1, airfoil application knowledge	Conducted alongside Objective 1; rapid analysis once data is available.
Investigate Stall Behavior	1 week	XFLR5 software, computational resources, data analysis skills	Focus on determining stall angle and basic lift/drag analysis.
Provide a Comparative Analysis of Performance Metrics	0.5 week	Data from Objectives 1 & 3, Excel/spreadsheet software	Focus on key performance values for efficiency.
Document and Visualize Results	0.5 week	Data visualization tools (Excel)	Prioritize clear, concise visualizations.

Tools Used:

- XFLR5 - v6.61

XFLR5 is an aerodynamic analysis tool primarily used for studying airfoils, wings, and aircraft at low speeds. It is based on the XFOIL engine for airfoil analysis and extends its capabilities using methods like the Lifting Line Theory, Vortex Lattice Method (VLM), and 3D panel methods for wing and aircraft evaluations. XFLR5 allows users to visualize flow characteristics, pressure distribution, lift, drag, and stability parameters. It is widely used in academia and research for conceptual aircraft design, UAV development, and aerodynamic performance optimization due to its user-friendly interface and detailed graphical outputs.

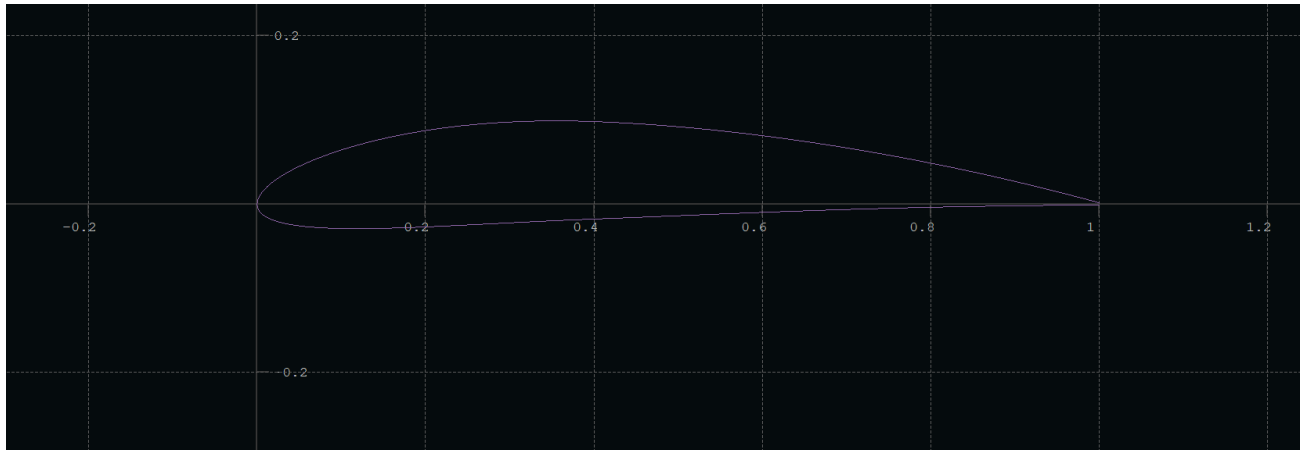
- Excel- For graph visualization.
- Word - For documentation.

Geometry Import and Setup:

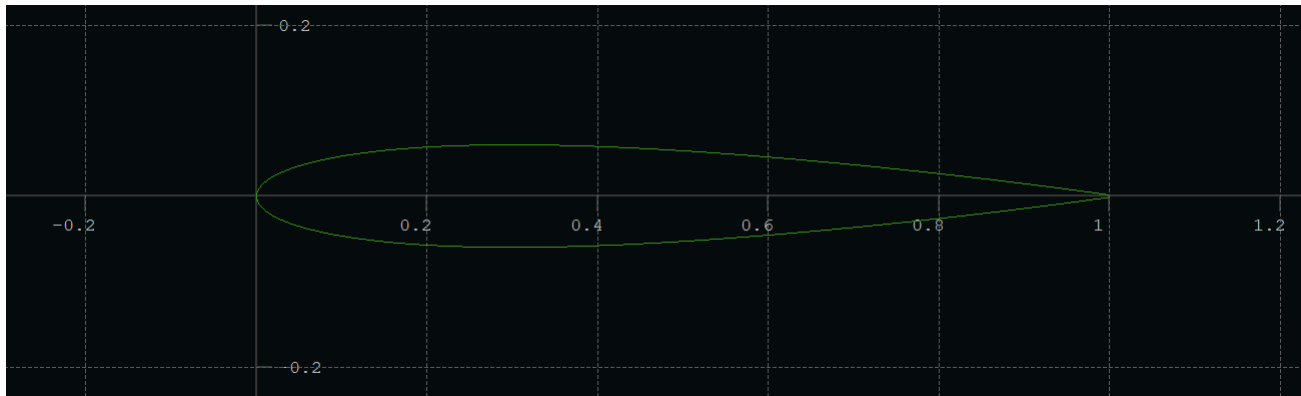
I. Import airfoil profiles (NACA 4412 and NACA 0012):

Foils are loaded from standard foil files and are stored in a runtime database.

1. **Low-Speed Aircraft Airfoil:** NACA 4412 (high camber, suited for low-speed, high-lift applications).



2. **High-Speed Aircraft Airfoil:** NACA 0012 (symmetrical airfoil, suited for high-speed, low-drag applications).



II. Geometry Setup:

The Geometrical Setup for both airfoils are quite simple. It defines the physical parameters of the airfoil, including chord length and thickness distribution. These parameters establish the fundamental shape characteristics that determine the airfoil's aerodynamic performance and structural properties.

Step-by-Step Procedure for Airfoil Design:

1. Launch XFLR5
2. Click on Module.
3. Click on Direct Foil Design.
4. Click on Foil.
5. Click on NACA Foils.
6. Enter the 4 Digit series number (Example: 0012/4412).
7. Click on OK.

III. Define analysis parameters:

- **Reynolds number** (e.g., 500,000 for low-speed, 2,000,000 for high-speed).
- **Angles of attack: -5° to 15° for low-speed and -2° to 10° for high-speed.**

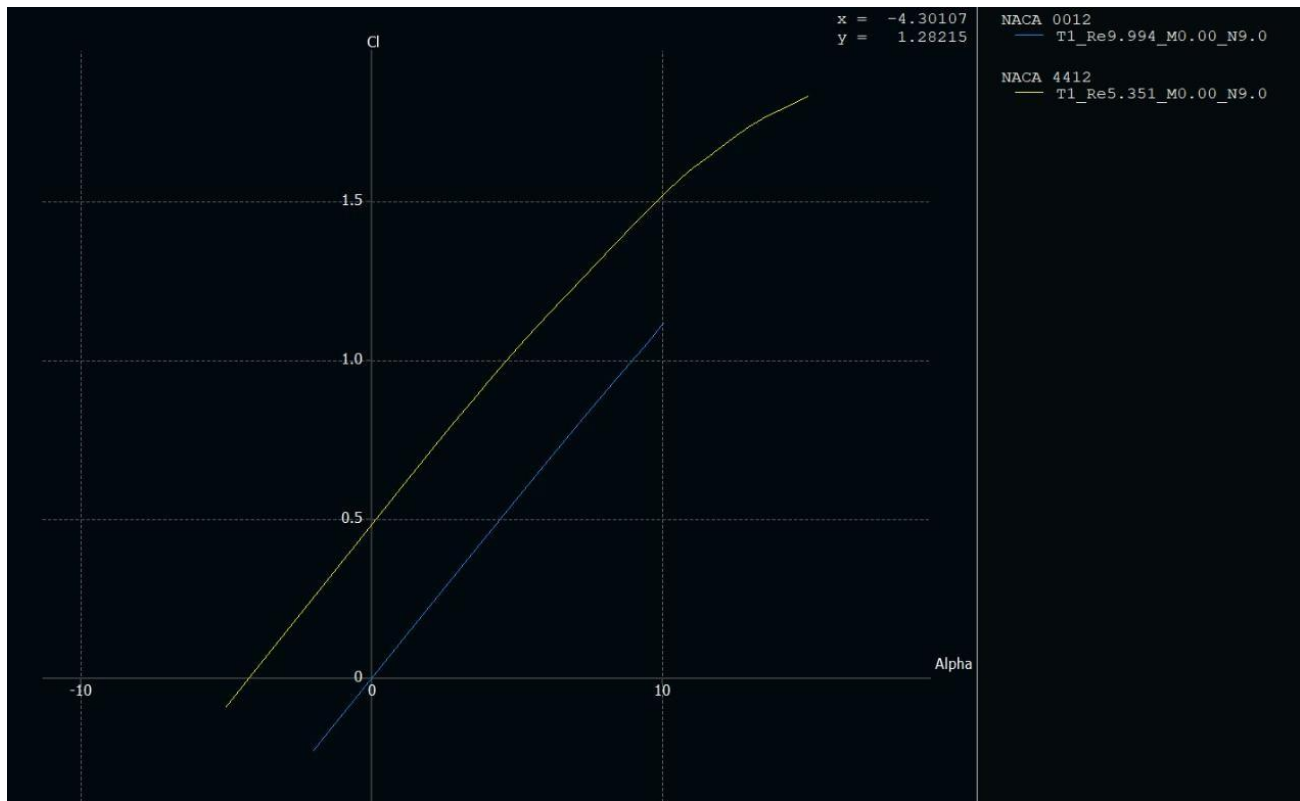
For the NACA 4412 airfoil, a Reynolds number of **5,351,123**(Aeronca 11CC Superchief)[\[5\]\[8\]](#) was utilized, representing low-speed operational conditions. In contrast, the NACA 0012 airfoil was evaluated at a Reynolds number of **9,993,823**(T-6 Texan)[\[4\]\[8\]](#) simulating high-speed flight regimes. The angle of attack ranges were similarly differentiated between the two airfoils: NACA 4412 was analyzed across a broader spectrum from -5° to 15°, while NACA 0012 was examined within a more conservative range of -2° to 10°. These parameters were selected to accurately represent the distinct operational characteristics and performance envelopes of each airfoil design.

Step-by-Step Procedure for Reynolds number & AoA definition:

1. Click on **Module**.
2. Select **XFoil Direct Analysis**.
3. Choose **NACA 0012** in **Object Explorer**.
4. Click on **Analysis**.
5. Select **Define an Analysis**.
6. Choose **Reynolds Number** in **Type 1**, i.e., **9,993,823** (for High-Speed Aircraft Airfoil).
7. Click on **OK**.
8. In **Direct Foil Analysis**, click on the **Sequence**, **Init BL**, and **Store Opp** checkboxes.
9. Assign the **Start** and **End** values as **-2 to 10 degrees (AoA)** [Adjust **Delta** if required].
10. Click on **Analyze**.
11. The graphs are generated for the **NACA 0012 Airfoil**.
12. Now, choose **NACA 4412** and repeat the same steps from **4 to 10**, with **Reynolds Number 5,351,123** and **AoA as -5 to 15 degrees for Start and End**, respectively (for Low-Speed Aircraft Airfoil).
13. Click on **Analyze**.
14. Similarly, the graphs are generated for the **NACA 4412 Airfoil**.

Graphs generated (Y vs X Orientation):

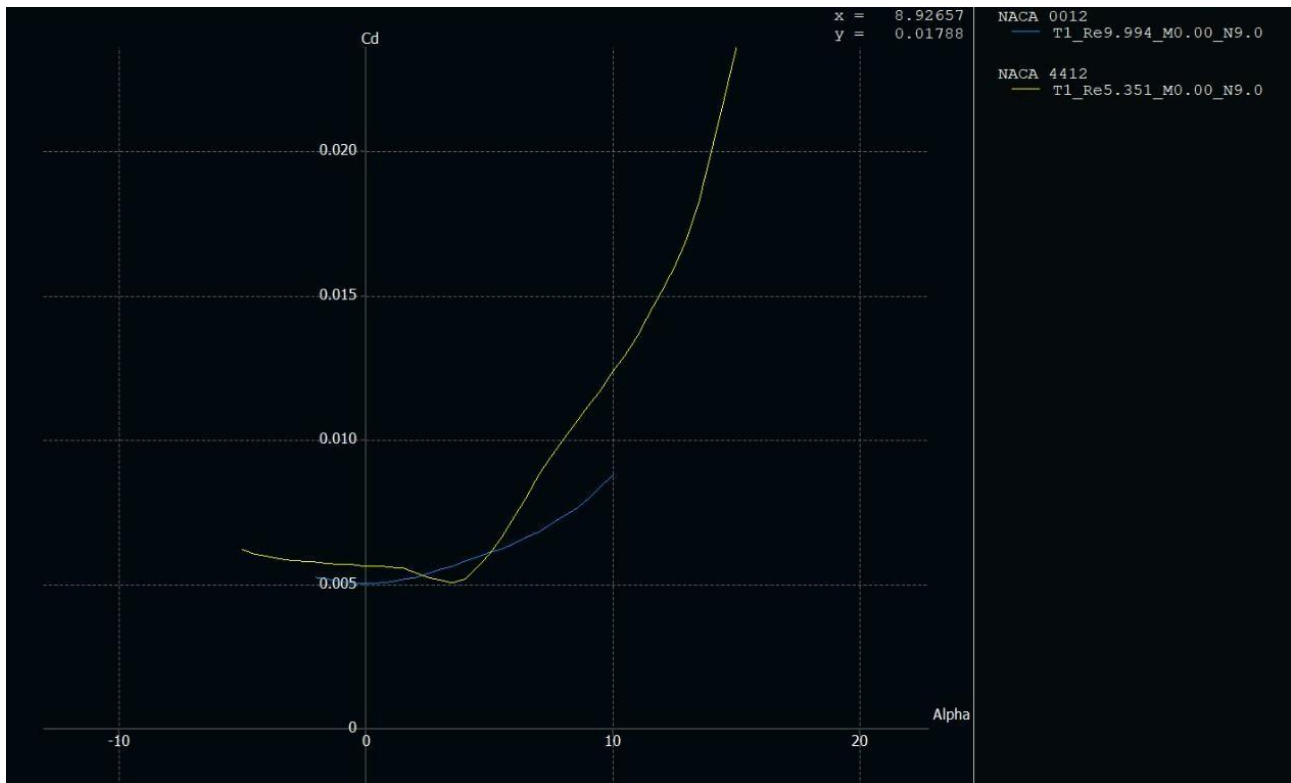
1. Lift coefficient (Cl) vs. Angle of attack (α) for both airfoils:



OBSERVATION:

1. Both curves show a nearly linear increase in lift up to a certain angle, beyond which stall might occur. The higher Reynolds number for NACA 0012 indicates better aerodynamic efficiency at higher speeds.
2. Both airfoils exhibit the expected trend of increasing lift with angle of attack, eventually leading to a stall. The graph doesn't show the full stall, but we can infer that it occurs beyond the plotted range.
3. The NACA 4412 consistently generates more lift than the NACA 0012 at the same positive angle of attack. This highlights the lift-enhancing effect of camber.
4. While the focus is on positive angles, the trend suggests that the NACA 0012 might have a more symmetrical lift profile around zero angle of attack compared to the NACA 4412. This is due to the inherent lift bias of cambered airfoils.

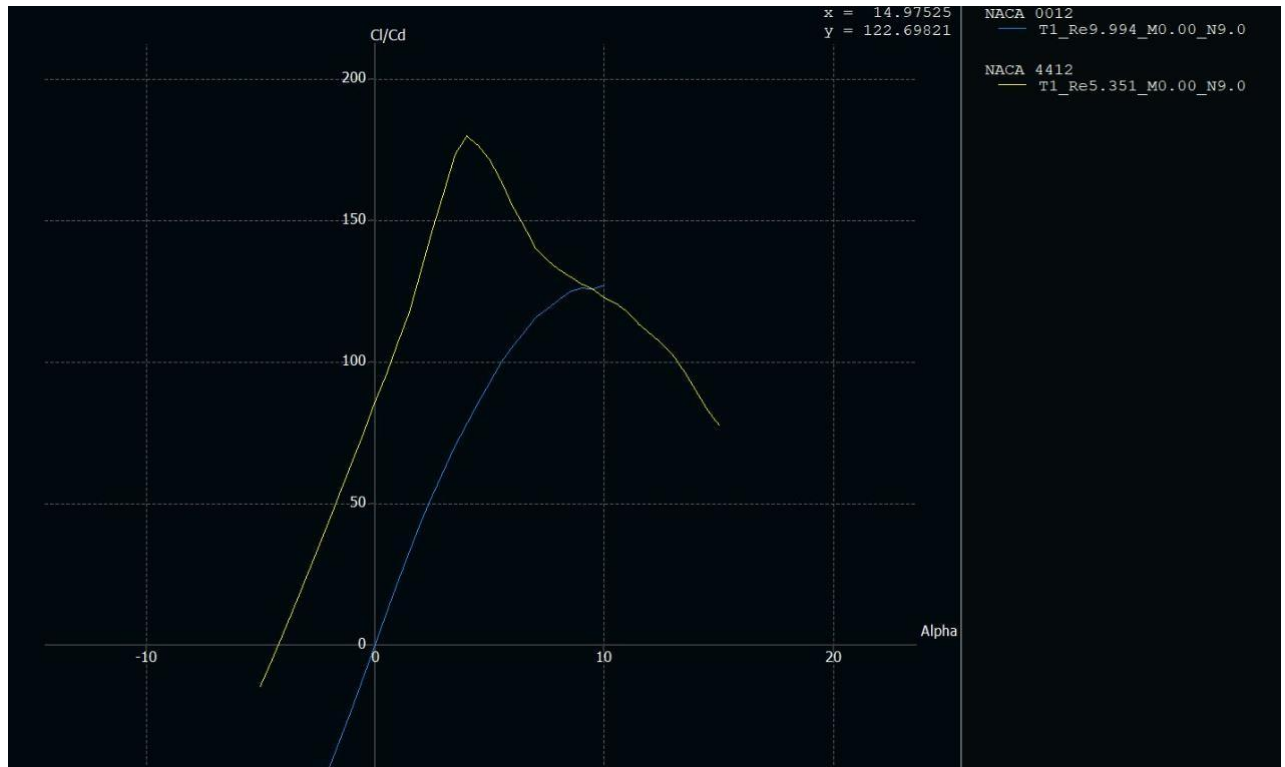
2. Drag coefficient (C_d) vs. Angle of attack (α) for both airfoils:



OBSERVATION:

1. Both airfoils show an increase in drag coefficient (C_d) as the angle of attack (α) increases. However, the rate of increase is not uniform.
2. At lower angles of attack (around 0 degrees), the NACA 0012 (purple line) exhibits a slightly higher drag coefficient compared to the NACA 4412 (yellow line).
3. Both airfoils exhibit a minimum drag coefficient at a slightly positive angle of attack. The NACA 4412's minimum drag occurs at a slightly higher angle of attack compared to the NACA 0012.
4. The NACA 4412 also shows an increase in drag with increasing angle of attack, but the rise is less steep compared to the NACA 0012 within the plotted range.

3. Lift-to-drag ratio (Cl/Cd) vs. Angle of attack (α):



OBSERVATION:

1. Both airfoils show an initial increase in Cl/Cd with increasing angle of attack, reach a peak value, and then experience a decrease.
2. The NACA 0012 (purple line) achieves a significantly higher peak Cl/Cd ratio compared to the NACA 4412 (yellow line).
3. The NACA 4412 reaches its peak Cl/Cd at a lower angle of attack compared to the NACA 0012.
4. The Cl/Cd ratio for both airfoils decreases after reaching their peak values. The decrease is particularly sharp for the NACA 4412.



AERONCA 11CC SUPERCHIEF:

Design and Development:

Aeronca was noted for producing light side-by-side two-seat touring aircraft since the introduction of the Aeronca C-2 in 1929. A more refined aircraft with an improved undercarriage and steel tube wing bracing struts in place of wires, was developed in 1937 as the Aeronca K, powered by a 42 hp (31 kW) Aeronca E-113 engine, beginning the

long line of Aeronca high wing touring, training, military liaison and observation aircraft of the 1930s and 1940s. The K series was powered by a variety of 40 hp (30 kW) to 50 hp (37 kW) Aeronca, Continental, Franklin or Menasco engines.[\[5\]](#)

Consumer demand for more comfort, longer range and better instrumentation resulted in development of the Aeronca 50 Chief in 1938. Although little more than an incremental development of the K series the Model 50 heralded a new designation system used for the high-winged tourers, including the manufacturer and power rating of the engine, dropping the letter designation system. Thus, the Aeronca 65CA Super Chief was powered by a 65 hp (48 kW) Continental A-65 with side-by-side seating and improvements over the 65C Super Chief. Other developments included tandem seating for use as trainer, liaison, observation aircraft or glider trainers as well as float-plane versions. Throughout the production life of the Aeronca Chief family the aircraft was improved incrementally, from a rather basic specification to a reasonably comfortable tourer with car-style interior.[\[5\]](#)

Description:

The Aeronca high-wing formula used a welded steel tube fuselage covered with fabric, wooden wings covered with plywood and fabric braced by V-struts to the rear undercarriage attachment point on the lower fuselage. Tail surfaces were also built up with welded steel tubing covered with fabric. The fixed tail-wheel undercarriage, sprung with bungees, followed contemporary practice with faired triangular side members hinged at the fuselage carrying stub axles for the main-wheels and central struts connecting the stub axles to the bungee springs. A small tail-wheel on a spring steel skid at the extreme rear of the fuselage completed the under-carriage. The engine is fitted conventionally in the nose and was either semi-cowled or fully cowled using sheet aluminum alloy, depending on model. Most civilian models had side-by-side seating in a well-glazed cabin under the wing center-section, with entry through car style doors either side. A tandem seating arrangement was developed for training and military models with the rear seat mounted 9 in (229 mm) inches higher than the front to allow the instructor to use the same instruments as the trainee and improve forward view from the back seat. Tandem seat aircraft had extensively glazed cockpits to allow good all-round visibility.[\[5\]](#)

A wide variety of engines were available for use on the Aeronca Chief series, including home grown Aeronca engines and Continental, Franklin, Menasco or Lycoming engines. The engine installed was reflected in the designation using the initial letter as a suffix in the designation.

Aeronca continued development during World War II, introducing the tandem seating Aeronca 7 Champion, taking advantage of the refinements developed with previous versions.



T-6 TEXAN:

Design and Development:

The T-6 Texan originated from the North American NA-16 prototype, first flown in 1935. It was modified into the NA-26 and submitted for a USAAC "Basic Combat" aircraft competition in 1937. The first production models were designated BC-1 and supplied to the USAAC, while the British RAF received them as the Harvard I. The US Navy operated a modified version called the SNJ-1. The

AT-6 version featured new outer wing panels with a swept-forward trailing edge, squared-off wingtips, and a triangular rudder, defining the Texan's iconic look. The AT-6 was later designated the Harvard II for RAF and RCAF orders. Over 1,173 units were supplied via purchase or Lend-Lease, primarily serving in Canada.[\[4\]](#)

Subsequent models, such as the AT-6A, were powered by the Pratt & Whitney R-1340-49 Wasp radial engine. The USAAC received 1,549 units, while the US Navy received 270 under the SNJ-3 designation. Canada's Noorduy Aviation built the AT-16 Harvard IIB, with over 2,485 aircraft produced. The Japanese Imperial Navy also acquired two NA-16s for study, leading to the K10W1 (Oak), though it bore little resemblance to the T-6. The NA-88 design further improved the Texan, resulting in the AT-6C, AT-6D, and SNJ-4 variants, with the Harvard III and Harvard 4 being among the final evolutions. Over 15,495 T-6 Texans were built across different versions, serving various air forces, including the USAAF, RAF, RCAF, and Bundeswehr during and after World War II.

Description:

The North American T-6 Texan was a game-changing military trainer aircraft developed from the NA-16 prototype in the 1930s. Designed with a low-wing configuration, enclosed tandem cockpit, and a Pratt & Whitney R-1340 "Wasp" radial engine, it provided the perfect balance between durability and performance. Its all-metal construction allowed it to endure rigorous training while offering flight characteristics that were challenging yet forgiving, making it an ideal transition between primary trainers and high-performance combat aircraft.

During World War II, the T-6 saw massive production and global use under different names: AT-6 (U.S. Army Air Forces), SNJ (U.S. Navy), and Harvard (British Commonwealth forces). It featured a standardized cockpit layout, preparing pilots for frontline aircraft, and its tandem seating arrangement allowed instructors to guide trainees effectively. The Texan played a crucial role in training pilots for aerobatics, formation flying, instrument navigation, and even weapons deployment, setting a new standard for military flight instruction.[\[4\]](#)

Post-war, the T-6 remained in service with numerous air forces worldwide, with some variants adapted for light attack and counter-insurgency roles by adding machine guns and light ordnance. Even after its military retirement, many T-6s were preserved as warbirds, continuing to fly in airshows and historical exhibitions. Its enduring legacy cements its status as one of the most influential trainer aircraft in aviation history.

Aerodynamic Simulations:

Performance Analysis:

XFOil provides unique insight in the behaviour of airfoils, but is a 2D analysis, hence the results are those of a wing of infinite aspect ratio and which is defined with a single airfoil. The influence that the aspect ratio alone may have on the wings polars, let alone the sweep or the dihedral, justifies the need for a more sophisticated wing analysis. The wing may be computed by either one of three methods, each having its own advantages, and all having some usage restrictions. The first is a **Lifting Line method**, derived from **Prandtl's wing theory**. The second is a **Vortex Lattice method**. The third is a **3D panel method**. The originality of the implementations is their coupling with XFOil calculation results to estimate the viscous drag associated with the wing, although this is done in a different manner depending on the method. In this project we will use **VLM method**.[\[7\]](#)

Here are some reasons for it:

The calculation of the lift distribution, the induced angles and the induced drag is **inviscid and linear** i.e. it is independent of the wings speed and of the air's viscous characteristics.

The method is applicable to any usual wing geometry, including those with sweep, low aspect ratio or high dihedral, including winglets.

NACA 0012:

Application considered: **T-6 TEXAN** [\[4\]](#)

Reason:

1. Reduced C_d makes it efficient at high Reynolds numbers.
2. Suitable for high-speed stability rather than slow-speed maneuverability.
3. Symmetric design prevents unnecessary pitching at high speeds.
4. Maintains necessary lift while minimizing drag for smooth flight.

MASS CALCULATION:

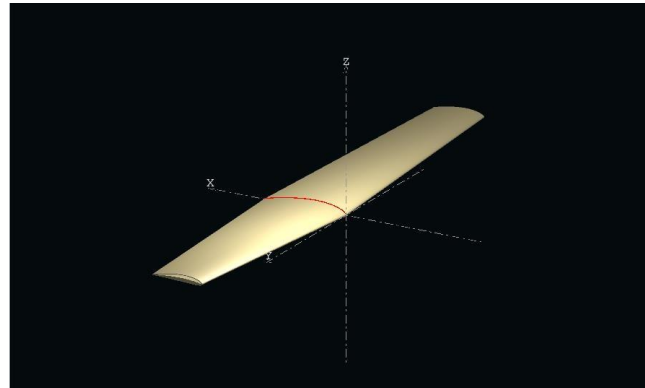
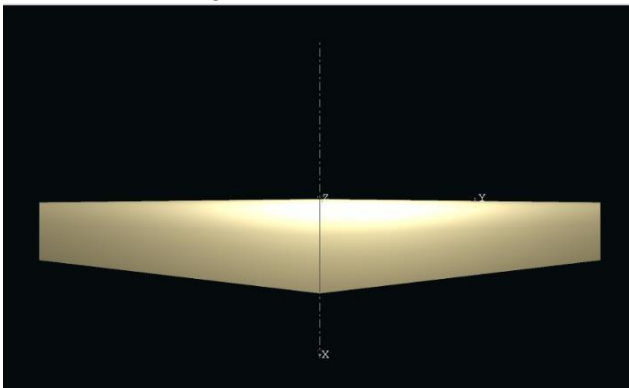
The wing mass is determined based on the wing area (S) (sq ft), maximum take-off weight (W_{total}) (lbs), and an empirical constant (0.04).[\[3\]](#) (chapter15)

The Formula is $m_{wing} = 0.04 \times S \times \sqrt{W_{total}}$ where, $S = 253.7$ sqft, $W_{total} = 5617$ lb
So, $m_{wing} = 760.55$ lbs \rightarrow **344.97 kg**

m_{wing} = mass of the wing
 W_{total} = Maximum Takeoff weight
Empirical constant = 0.04

Step-by-Step Procedure for Defining a Wing:

1. **Open Module** → Select **Wing and Plane Design**.
2. **Click on Plane** → Define a new plane.
3. **Uncheck** Elevator and Fin checkboxes → Name the plane **T-6 TEXAN**
4. Click **Define** in the **Main Wing Component**.
5. In the new window:
 - a. Under the **Foil** column, select **NACA 0012** (both rows).
 - b. Set **Dihedral Angle** to 5° .
6. Click **Other** in the **Description Toolbar** → Select **Inertia**.
7. Enter **Wing Mass: 344.97 kg** (as Calculated above) → Click **Save**.
8. Click **Other** again → Select **Scale Wing**.
9. Adjust:
 - a. **Span Scaling:** 13m
 - b. **Area Scaling:** 23.57m^2
 - c. **Aspect Ratio Scaling:** 7.17
10. Click **OK** → Modify, **Offset [Croot-Ctip/WingSpan]**.
11. Click **Save** → Click **Save** again.
12. **Click Module** → **Direct Foil Analysis**.
13. **Click Analysis** → Select **Batch Analysis**.
14. Choose **NACA 0012 Airfoil**.
15. Set **Alpha Min = -2**, **Alpha Max = 10** → Click **Analyze**.
16. Polars are generated → Click **Close**.



Step-by-Step Procedure for 2D Inviscid Analysis:

1. **Open Module** → Select **Wing and Plane Design**.
2. **Click Analysis** → **Define New Analysis**.
3. Under **Polar Type**, Set **Velocity** to 64.8m/s (Cruise Speed).
4. Click **Analysis**, select **Ring Vortex VLM 2**.
5. In **Inertia & Reference Dimensions**, verify values:
 - a. If correct → Click **Save**.
 - b. If incorrect → Adjust values → Click **Save**.
6. In **Plane Analysis Settings**:
 - a. Check Sequence Box, InitLLT, Store OpPoint.
 - b. Set **Start = -2**, **End = 10**, **Delta = 0.5**.
 - c. Click **Analyze**.
7. Graphs are generated.

Step-by-Step Procedure for 2D Viscous Analysis:

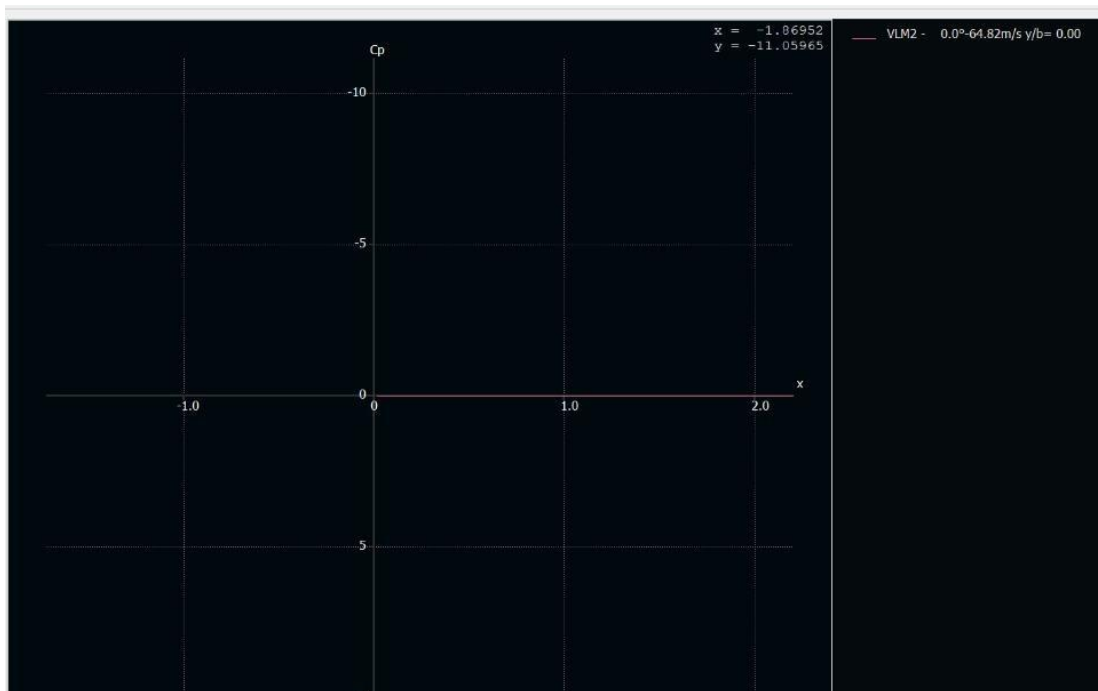
1. Perform steps 1-4 again with the same selections and settings as above.
2. In the same tab, check the **Viscous** checkbox.
3. Perform steps 5-7 again with the same selections and settings as above.

NOTE: The structural design of the wings must support the full aircraft weight, including fuel, payload, and passengers. The wing's mass depends on how much total lift it must generate, which is linked to the maximum weight the aircraft is expected to carry.

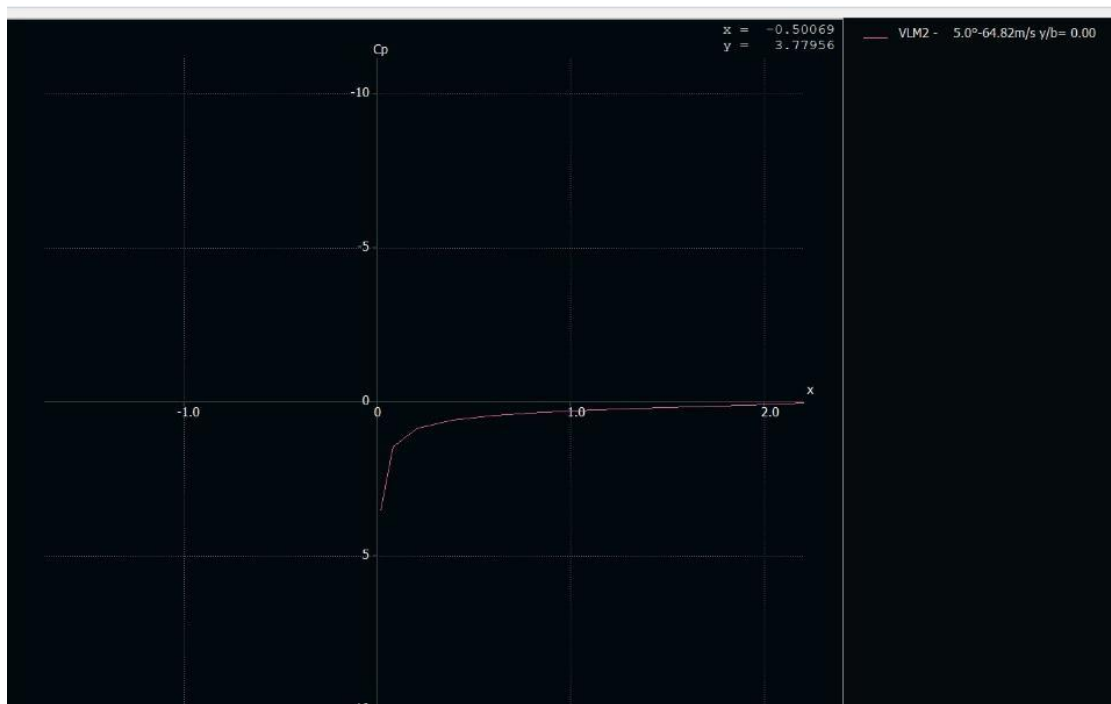
Graphs generated (Y vs X Orientation):

4. Pressure coefficient (C_p) distribution at key angles of attack for NACA 0012 (at 0° , 5° , 10° respectively):

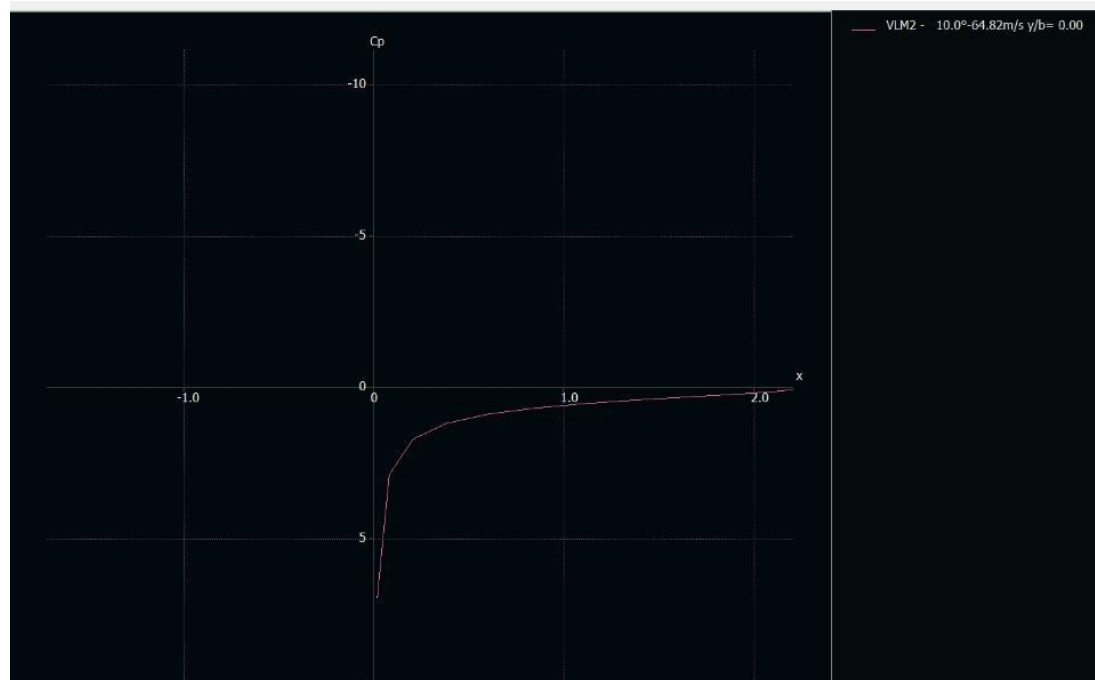
i) At 0 degrees (Overlapping about X-axis):



ii) At 5 degrees:



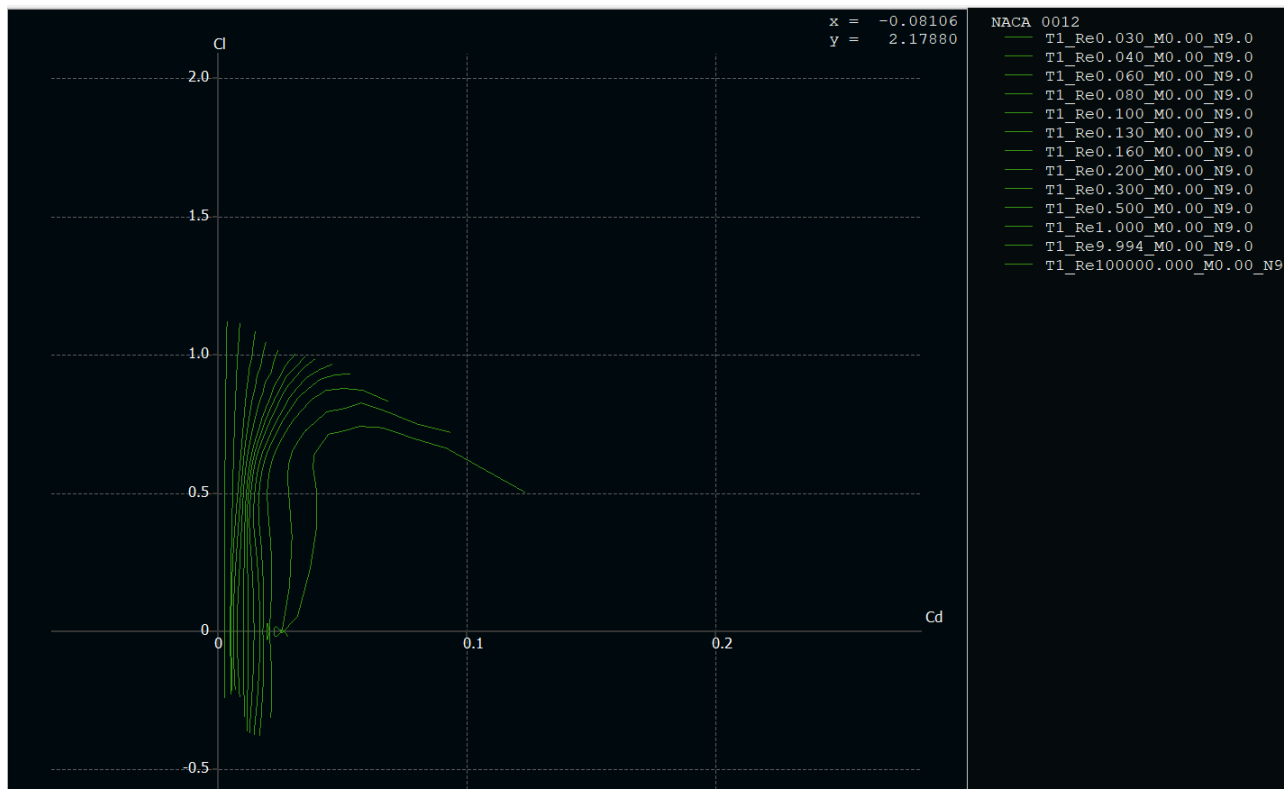
iii) At 10 degrees:



OBSERVATION:

1. **At 0° angle of attack**, the pressure distribution remains nearly uniform across the airfoil, with minimal difference between the upper and lower surfaces. The coefficient of pressure (C_p) curve is relatively flat, indicating negligible lift production. There is only a slight negative pressure on the upper surface, leading to no significant aerodynamic force generation
2. **At 5° angle of attack**, a noticeable negative pressure peak appears on the upper surface near the leading edge, while the lower surface experiences increased positive pressure. This pressure differential results in significant lift generation. The C_p curve shows a clear separation between the upper and lower surfaces, indicating a well-established pressure difference responsible for lift.
3. **At 10° angle of attack**, the negative pressure peak on the upper surface becomes even more pronounced, and the positive pressure on the lower surface increases further. This results in a stronger pressure differential and greater lift. The C_p curves show a more significant gap between the upper and lower surfaces, highlighting the increased aerodynamic force. Additionally, the center of pressure shifts slightly forward as the angle of attack increases.

5. Polar plots (C_l vs. C_d) for NACA 0012 airfoil:



OBSERVATION:

1. Higher Reynolds numbers generally produce better aerodynamic efficiency (higher lift-to-drag ratios), shown by curves reaching farther to the left.
2. Drag remains relatively low across a range of lift coefficients before increasing rapidly.
3. The maximum lift coefficient varies with Reynolds number, with higher Reynolds numbers generally achieving higher C_l values before stall (approximately 1.1 for the highest Re).
4. At very low Reynolds numbers (0.03-0.06 million), the airfoil exhibits poor performance with higher drag and limited lift capability.

NACA 4412:

Application considered: **Aeronca 11CC Super Chief** [\[5\]](#)

Reason:

1. Provides sufficient lift for short takeoffs and stable landings.
2. Higher stall angle allows better low-speed maneuverability.
3. Increased drag is acceptable due to the need for better lift.
4. Negative moment coefficient (C_m) ensures better control at low speeds.

MASS CALCULATION:

The wing mass is determined based on the wing area (S) (sq ft), maximum take-off weight (W_{total}) (lbs), and an empirical constant (0.04).[\[3\]](#)

The Formula is $m_{wing} = 0.04 \times S \times \sqrt{W_{total}}$ where,

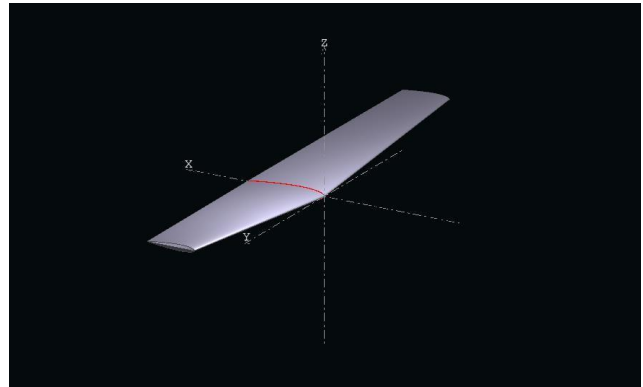
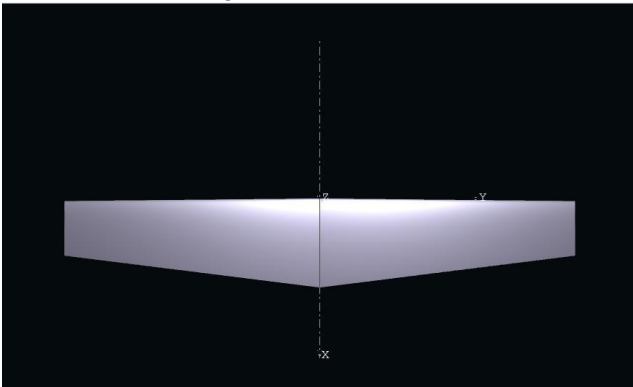
$S = 175$ sqft, $W_{total} = 1,350$ lb

So, $m_{wing} = 257.19$ lbs \rightarrow **116.66 kg**

Step-by-Step Procedure for Defining a Wing:

1. **Open Module** \rightarrow Select **Wing and Plane Design**.
2. **Click on Plane** \rightarrow Define a new plane.
3. **Uncheck** Elevator and Fin checkboxes \rightarrow Name the plane **Aeronca11CC Super Chief**.
4. Click **Define** in the **Main Wing Component**.
5. In the new window:
 - a. Under the **Foil** column, select **NACA 4412** (both rows).
 - b. Set **Dihedral Angle** to **3°**.

6. Click **Other** in the **Description Toolbar** → Select **Inertia**.
7. Enter **Wing Mass: 116.66kg** → Click **Save**.
8. Click **Other** again → Select **Scale Wing**.
9. Adjust:
 - a. **Span Scaling:** 11 m
 - b. **Area Scaling:** 16.3m²
 - c. **Aspect Ratio Scaling:** 7.426
10. Click **OK** → Modify **Offset Above Wing [Croot-Ctip/WingSpan]**.
11. Click **Save** → Click **Save** again.
12. Click **Module** → **Direct Foil Analysis**.
13. Click **Analysis** → Select **Batch Analysis**.
14. Choose **NACA 4412 Airfoil**.
15. Set **Alpha Min = -5, Alpha Max = 15** → Click **Analyze**.
16. Polars are generated → Click **Close**.



Step-by-Step Procedure for 2D Inviscid Analysis:

1. Click **Analysis** → **Define New Analysis**.
2. Set **Polar Type Velocity** to **42.5m/s** (cruise speed).
3. Under **Analysis Option**, select **Ring Vortex VLM 2**.
4. In **Inertia & Reference Dimensions**, verify values:
 - a. If correct → Click **Save**.
 - b. If incorrect → Adjust values → Click **Save**.
5. In **Plane Analysis Settings**:
 - a. Check **Sequence Box**.
 - b. Set **Start = -5, End = 15, Delta = 0.5**.
 - c. Click **Analyse**.
6. Graphs are generated.

Step-by-Step Procedure for 2D Viscous Analysis:

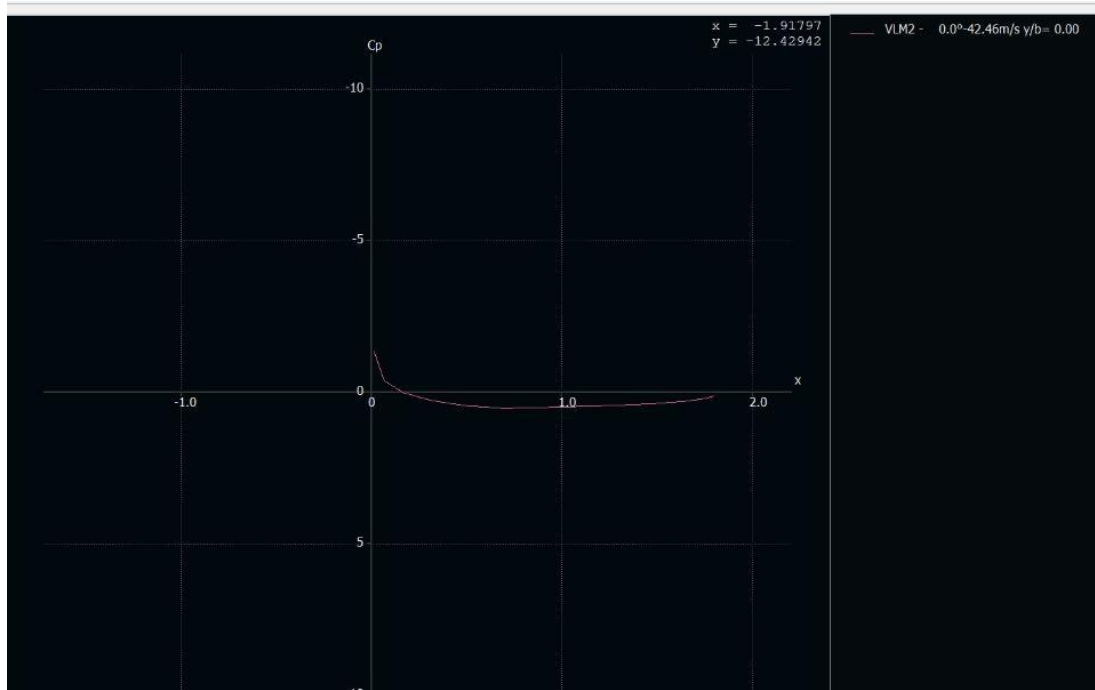
1. Perform steps 1-4 again with the same selections and settings as above.
2. In the same tab, check the **Viscous** checkbox.
3. Perform steps 5-7 again with the same selections and settings as above.

NOTE: The structural design of the wings must support the full aircraft weight, including fuel, payload, and passengers. The wing's mass depends on how much total lift it must generate, which is linked to the maximum weight the aircraft is expected to carry.

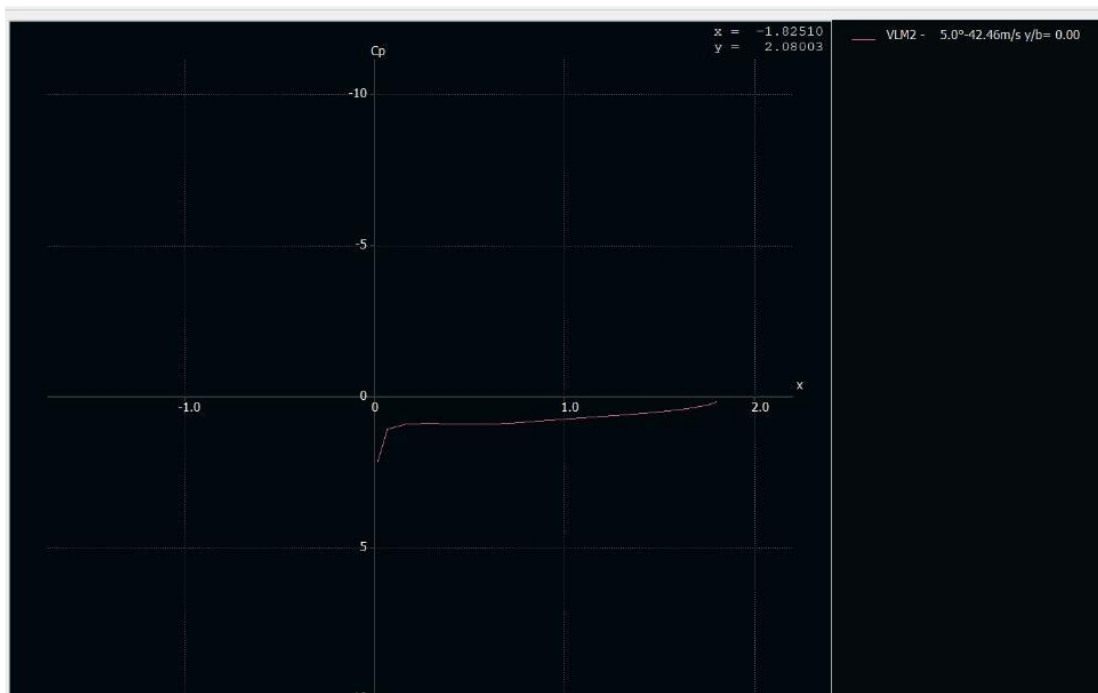
Graphs generated (Y vs X Orientation):

4. **Pressure coefficient (C_p) distribution at key angles of attack for NACA 4412 (at 0° , 5° , 10° respectively):**

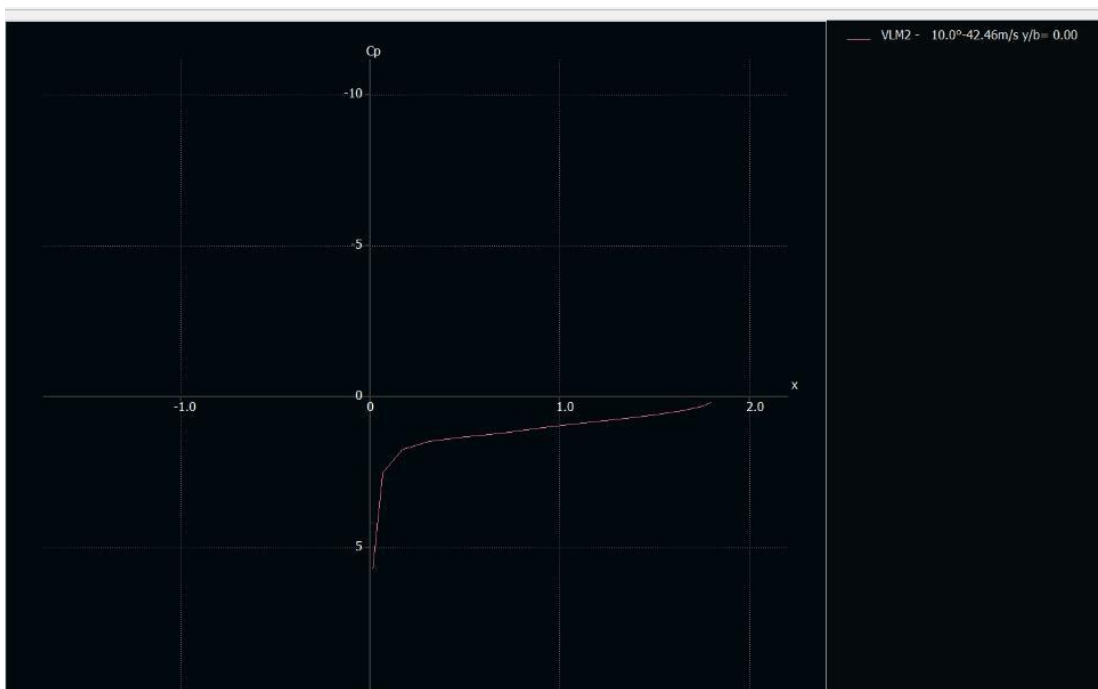
i) **At 0 degrees:**



ii) At 5 degrees:



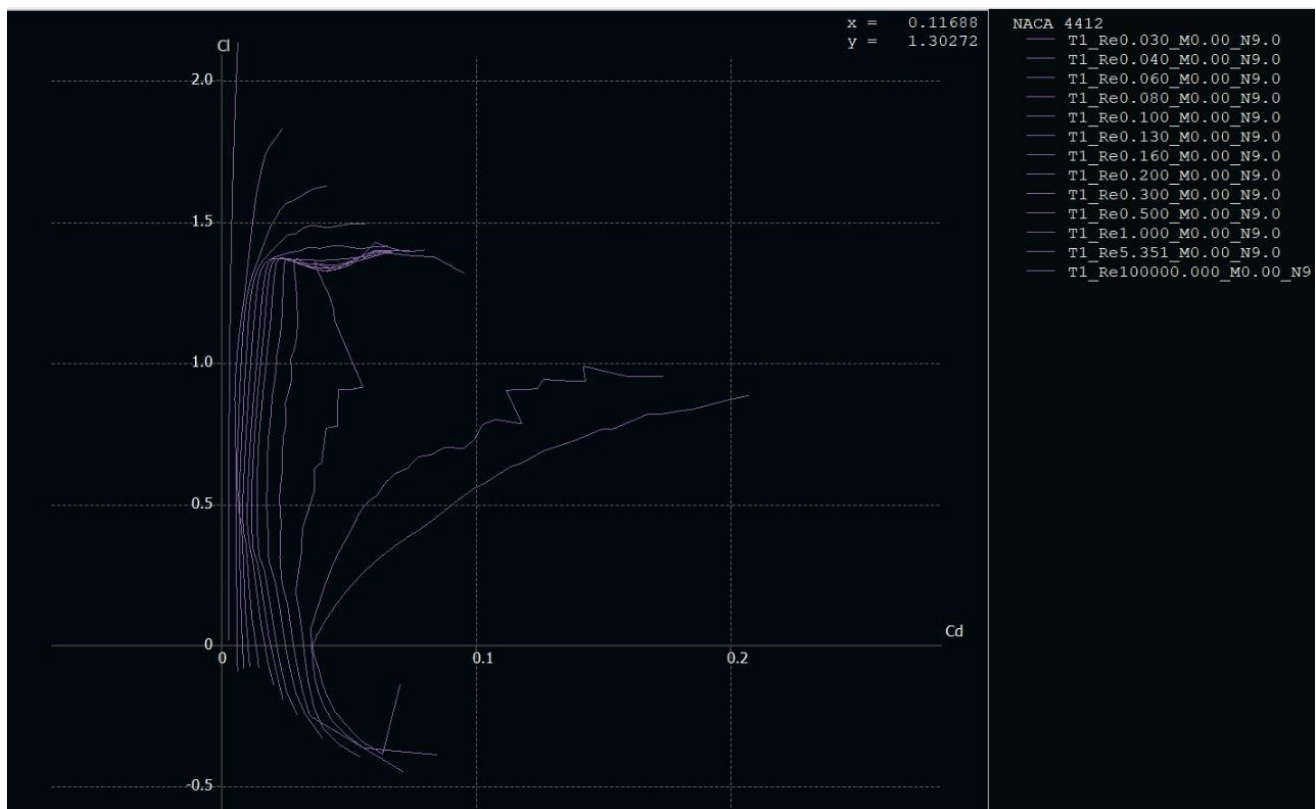
iii) At 10 degrees:



OBSERVATION:

1. **At 0° angle of attack**, the pressure distribution shows minimal difference between upper and lower surfaces, resulting in negligible lift production. The curve is relatively flat with only slight negative pressure on the upper surface.
2. **At 5° angle of attack**, a significant negative pressure peak develops on the upper surface near the leading edge, while positive pressure forms on the lower surface. This pressure differential generates substantial lift, visible in the clear separation between upper and lower surface pressure curves.
3. **At 10° angle of attack**, the pressure differential intensifies dramatically with a stronger negative pressure peak on the upper surface and increased positive pressure below. This creates greater lift force, evident in the more pronounced separation between the curves. The center of pressure also shifts forward as angle of attack increases.

5. Polar analysis to generate lift-drag for NACA 4412 airfoil:



OBSERVATION:

1. The NACA 4412 achieves higher maximum lift coefficients (up to ~1.8-2.0) compared to the NACA 0012, due to its cambered profile.
2. Unlike the symmetric NACA 0012, the 4412 shows distinct differences between positive and negative lift regions, with better performance at positive lift coefficients.

3. Performance improves significantly with increasing Reynolds numbers, with dramatic differences between low Re ($<0.1M$) and high Re values.
4. The airfoil maintains reasonable performance in the negative lift region, though with higher drag than in the positive region.

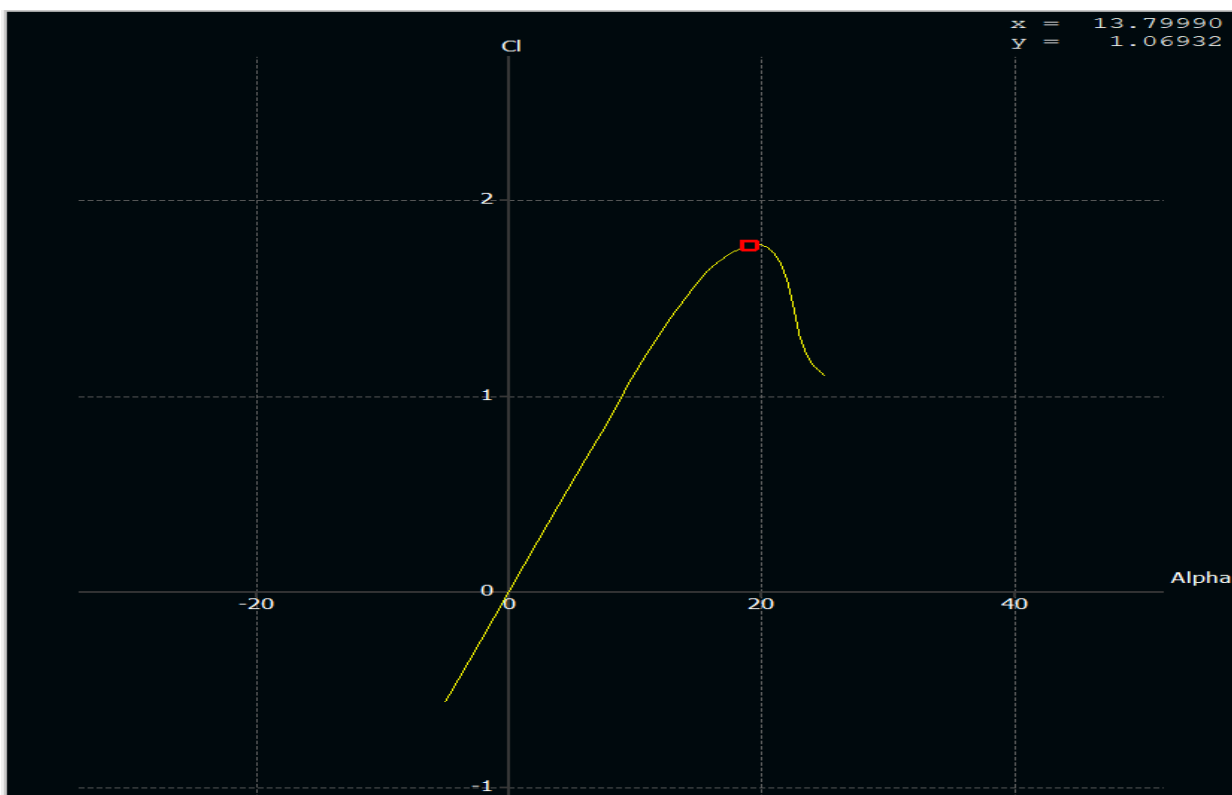
Stall Behaviour Analysis:

Stall Analysis:

Stall behavior analysis examines how an aircraft's wing loses lift as the angle of attack (AoA) increases beyond the critical stall point. This is typically done by analyzing **lift coefficient (CL) vs. angle of attack**, where CL increases with AoA until reaching a peak, after which it sharply drops, indicating stall. Additionally, **drag coefficient (CD) vs. (CL)** helps in understanding efficiency loss. Stall characteristics depend on airfoil shape, Reynolds number, and flow separation patterns. Understanding stall behaviour is crucial for flight safety, as it helps predict control loss, recovery strategies, and aerodynamic performance.[\[7\]](#)

6. Stall behaviour visualization (e.g., CL vs. α with stall marked):

I.NACA 0012:

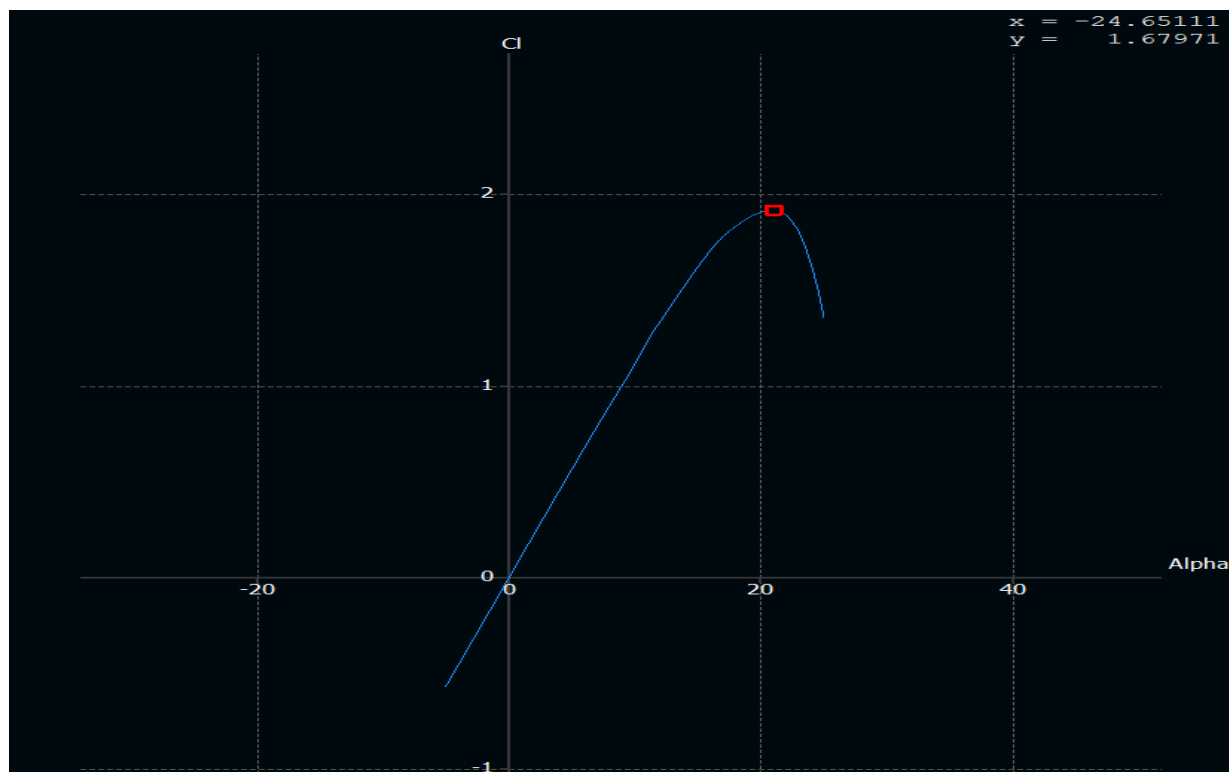


OBSERVATION:

The NACA 0012 airfoil exhibits a predictable aerodynamic profile with a stall angle of approximately 19 degrees. As the angle of attack increases from zero, the lift coefficient rises linearly, demonstrating good stability and predictable performance. This linear relationship continues until reaching the critical angle of attack at about 19 degrees, where the maximum lift coefficient is achieved.

At the stall point, boundary layer separation occurs as airflow can no longer follow the upper surface contour. Immediately after stall, the NACA 0012 experiences an abrupt decrease in lift coefficient, characteristic of thin, symmetric airfoils. This sharp drop indicates the airfoil's tendency toward sudden rather than gradual stall behaviour, which is an important consideration for aircraft design and handling properties.

II. NACA 4412:



OBSERVATION:

The NACA 4412 airfoil demonstrates a stall angle of approximately 20-21 degrees, as shown in the yellow curve. It exhibits a gradual lift increase with angle of attack, achieving a higher maximum lift coefficient than the NACA 0012. The cambered design of the 4412 airfoil contributes to its superior lift characteristics and slightly delayed stall point. After reaching its peak lift coefficient (marked by the red square at around 20-21 degrees), the airfoil experiences flow separation and a subsequent decrease in lift, though the post-stall behaviour appears somewhat less abrupt than the NACA 0012.

7. Moment coefficient (C_m) vs. Angle of attack (α) for stability analysis:



OBSERVATION:

The graph compares the pitching moment coefficient (C_m) versus angle of attack (α) for two aircraft: the Aeronca 11 CC Superchief and the T-6 Texan. Both aircraft show a linear relationship between C_m and α , indicating consistent aerodynamic behavior and longitudinal stability, as the negative slopes suggest a nose-down tendency that helps restore the aircraft to its original angle. The Superchief, with a lower speed (42.5 m/s), has a more positive C_m at zero α , suggesting a higher nose-up tendency, and a steeper negative slope, indicating higher static longitudinal stability. In contrast, the Texan, flying at a higher speed (64.8 m/s), has a lower C_m at zero α and a shallower negative slope, implying less inherent stability but potentially greater maneuverability. These differences reflect variations in trim settings, design (such as wing airfoil and tail configuration), and speed effects on aerodynamic forces. The steeper slope of the Superchief suggests greater resistance to changes in angle of attack, making it more stable, while the Texan may be more agile but less stable. It highlights how speed and design influence longitudinal stability in these aircraft, with the Superchief being more stable overall.

Performance Metrics:

Key Aerodynamic Parameters and Comparison:

1. **Lift-to-Drag Ratio (L/D):** The ratio of the lift coefficient (C_L) to the drag coefficient (C_D), representing aerodynamic efficiency. A higher L/D ratio indicates better performance in terms of lift generation with minimal drag.
 - a. **T-6 Texan:** Achieves the highest L/D ratio of **31.65 at 4 degrees AoA**. This suggests that at this angle, the aircraft experiences the best balance of lift and drag, making it optimal for sustained flight.
 - b. **Aeronca 11CC Super Chief:** Records the highest L/D ratio of **31.28 at 1-degree AoA**, indicating that this aircraft achieves its peak aerodynamic efficiency at a lower angle of attack compared to the T-6 Texan.
(Refer to C_L/C_D vs AoA Graph in Performance metrics folder)
2. **Zero-Lift Drag Coefficient (C_{D0}):** The drag coefficient when lift (C_L) is zero, representing the inherent aerodynamic resistance of the aircraft without any lift contribution.
 - a. **T-6 Texan:** $C_{D0} = 0.005$, indicating a relatively low parasitic drag, which enhances its aerodynamic efficiency.
 - b. **Aeronca 11CC Super Chief:** $C_{D0} = 0.007$, slightly higher than that of the T-6 Texan, implying a marginally greater drag component when not generating lift.
(Refer to C_L vs C_D Graph in Performance metrics folder)
3. **Maximum Lift Coefficient ($C_{L_{max}}$):** The highest value of C_L before stall occurs, representing the maximum lift the airfoil can generate.
 - a. **T-6 Texan:** $C_{L_{max}} = 1.613$, indicating a moderate lift-generating capacity before stall.
 - b. **Aeronca 11CC Super Chief:** $C_{L_{max}} = 1.925$, which is higher than that of the T-6 Texan, suggesting better lift performance before stall.
(Refer Stall Angle Graphs on Pg No 19,20)
4. **Moment Coefficient (C_m):** Represents the pitching moment acting on an airfoil, which influences aircraft stability and control, C_m value corresponding to maximum L/D ratio.
 - a. **T-6 Texan:** $C_m = -0.049$ at **0 degrees AoA**, due to its symmetrical airfoil (NACA 0012), leading to balanced aerodynamic moments.
 - b. **Aeronca 11CC Super Chief:** $C_m = -0.034$ at **1-degree AoA**, where the L/D ratio is at its maximum, suggesting a slightly lower pitching moment compared to the T-6 Texan.
(Refer to C_m vs AoA Graph in Performance metrics folder)

Analysis:

Both the T-6 Texan and the Aeronca 11CC Super Chief showcase impressive aerodynamic efficiency, achieving very similar and high lift-to-drag ratios, though at slightly different angles of attack. The T-6 Texan peaks at an L/D of 31.65 at 4 degrees AOA, while the Aeronca 11CC Super Chief reaches 31.28 at a lower 1-degree AOA. In terms of drag, the T-6 Texan exhibits a slightly lower zero-lift drag coefficient, indicating marginally less parasitic drag. However, the Aeronca 11CC Super Chief demonstrates a significantly higher maximum lift coefficient ($C_{l\max}$), suggesting superior lift generation capability before stall compared to the T-6 Texan.

Considering pitching moment characteristics, both aircraft display negative moment coefficients, indicating static stability. The T-6 Texan has a C_m of -0.049 at 0 degrees AOA due to its symmetrical airfoil, whereas the Aeronca 11CC Super Chief has a C_m of -0.034 at its maximum L/D angle of 1 degree. Overall, while both aircraft are aerodynamically well-designed, the T-6 Texan has a slight advantage in drag and peak L/D, and the Aeronca 11CC Super Chief excels in maximum lift generation, with comparable pitching moment characteristics ensuring static stability for both.

Thus, the **T-6 Texan** favours high-speed efficiency, while the **Aeronca 11CC Super Chief** is better suited for low-speed, high-lift applications

Comparative Study:

1. Suitability for low speed vs. high-speed flight:

Feature	T-6 Texan	Aeronca 11CC Super Chief
Airfoil	A semi-symmetrical or cambered airfoil, balancing lift and efficiency while allowing aerobatic maneuvers and high-speed stability.	NACA 4412 (Cambered), optimized for high lift at low speeds. This results in a greater coefficient of lift at lower angles of attack, making it ideal for short takeoff and landing (STOL) operations.
Designed Speed Range	Optimized for higher speeds (WWII Trainer), with a high wing loading and streamlined design reducing drag, allowing for sustained high-speed flight.	Designed for lower speeds, allowing for operations in short fields. The high-lift airfoil and wing design improve efficiency at slow speeds but limit top-speed performance.
Lift-to-Drag Ratio (L/D)	Higher at moderate-to-high speeds, meaning less drag relative to lift, improving efficiency during cruise flight. At lower speeds, drag increases due to flow separation, affecting low-speed handling.	Optimized for high lift at low speeds, leading to better takeoff performance but at the cost of higher drag at cruising speeds. This trade off is beneficial for operations in short-runway environments.
Flaps	Equipped with flaps that improve low-speed handling, increasing lift and delaying stall onset, which helps with controlled landings.	Uses a high-lift wing and flaps designed specifically for STOL (short takeoff and landing), enhancing performance in confined spaces.
Overall Suitability	Excels in high-speed flight, making it suitable for training, combat, and high-speed maneuvering. However, stall speeds are higher compared to the Aeronca 11CC Super Chief.	Best suited for low-speed operations, particularly in short field landings and takeoffs, where its aerodynamic properties provide greater control and stability at lower speeds.

2. Sensitivity to Reynolds number:

Feature	T-6 Texan	Aeronca 11CC Super Chief
Reynolds Number Range	Higher (~5-10 million) due to its larger size and higher speeds, which increase aerodynamic forces and promote a fully turbulent boundary layer.	Lower (~1-5 million) due to its smaller size and slower speeds, where laminar flow plays a more significant role in lift and drag characteristics.
Effect on Performance	Less affected by changes in Reynolds number because the transition from laminar to turbulent flow happens at higher speeds, where the design is optimized. This provides stable performance in a wide range of conditions.	More affected by Reynolds number variations because laminar-to-turbulent transition can cause sudden changes in drag and lift, affecting overall performance at different speeds.
Flow Transition	Likely turbulent over most of the wing at operational speeds, which helps maintain stability but increases skin friction drag. The presence of turbulent flow allows for better control in high-speed flight.	More prone to laminar-to-turbulent transition issues, which can cause drag fluctuations and performance inconsistencies. At lower speeds, maintaining laminar flow is beneficial for efficiency, but when transition occurs, drag increases significantly.

3. Stability characteristics based on moment coefficients:

Feature	T-6 Texan	Aeronca 11CC Super Chief
Pitching Moment Coefficient (CM)	Slightly negative (-0.02 to -0.05), which means the aircraft has a mild nose-down tendency, contributing to stable flight and easy recovery from stalls.	More negative, meaning a stronger nose-down moment. This requires more pilot control to counteract, but it aids in stall recovery.
Center of Pressure Movement	More stable at higher speeds due to predictable aerodynamic forces. The center of pressure shifts slightly but remains manageable, ensuring stability.	Center of pressure shifts more noticeably at lower speeds, which can affect pitch stability, requiring more pilot adjustments.
Longitudinal Stability	More stable, allowing for better-controlled maneuvers. The aircraft naturally resists pitch disturbances, making it easier to fly at high speeds.	Requires more pilot correction at varying speeds because its aerodynamic design makes it more sensitive to external forces, especially in turbulent conditions.
Tailplane Influence	The tailplane provides consistent stability across all speeds, helping maintain level flight and smooth maneuvering.	The high-lift design of the wing makes the tailplane's influence more significant, leading to increased pitch sensitivity, especially at slow speeds.

Conclusion:

Why NACA 4412 is Best for Low-Speed Aircraft?

NACA 4412 is a **cambered airfoil**, which means its shape naturally generates **more lift at lower speeds**. The **higher lift coefficient** allows aircraft using this airfoil to achieve lift-off at lower velocities, making it ideal for **short take-off and landing (STOL) operations**. This is particularly beneficial for aircraft operating in small airfields, bush flying, or general aviation applications, where **low-speed efficiency** is crucial.

However, the **higher lift** comes at the cost of **increased drag**. The drag coefficient of NACA 4412 is **higher** than that of symmetric airfoils, particularly at **higher speeds**. This results in **greater energy loss** due to air resistance, limiting its efficiency for high-speed flight. Additionally, the more negative pitching moment coefficient causes a nose-down tendency, requiring the use of a stabilizer or trim adjustments to maintain level flight.

NACA 4412 is also **more sensitive to Reynolds number variations**, meaning that its performance changes significantly with variations in airspeed. At **lower Reynolds numbers**, laminar-to-turbulent transition occurs earlier, leading to **sudden changes in lift and drag**. Despite these limitations, the **high lift generation and slow-speed stability** of NACA 4412 make it the preferred choice for **low-speed aircraft** such as the **Aeronca 11CC Super Chief**, light sport aircraft, and small general aviation planes.

Why NACA 0012 is Best for High-Speed Aircraft?

NACA 0012 is a **symmetric airfoil**, meaning it has **no camber**. This results in **lower lift at lower speeds** but offers a significant advantage at higher speeds. The **lift-to-drag ratio** is much more favourable for high-speed flight, as the **lower drag coefficient minimizes resistance and improves efficiency**. This makes NACA 0012 the preferred airfoil for aircraft designed to **operate at high Reynolds numbers**, where the airflow remains attached to the surface for a longer duration, **reducing drag and improving stability**.

The **pitching moment coefficient** of NACA 0012 is close to zero, meaning the airfoil **does not naturally pitch up or down**, reducing the need for stabilizer adjustments. This **stability in high-speed flight** is crucial for aircraft that need to maintain precision during maneuvers, such as **trainers (e.g., T-6 Texan)**, aerobatic aircraft, UAVs, and high-speed military jets. Additionally, NACA 0012 is **less sensitive to Reynolds number changes**, meaning its aerodynamic performance remains consistent across different speed ranges, making it ideal for subsonic and transonic flight conditions.

Thus, while NACA 4412 is optimized for generating maximum lift at lower speeds, NACA 0012 is designed for minimal drag and stability at high speeds.

REFERENCES:

- [1] XFLR5, “XFLR5 Software Files,” SourceForge.
Available: <https://sourceforge.net/projects/xflr5/files/>. [Accessed: Feb.8,2025].
- [2] M. Selig, “Airfoil Coordinate Database,” University of Illinois at Urbana-Champaign.
Available: https://m-selig.ae.illinois.edu/ads/coord_database.html. [Accessed: Feb.9,2025].
- [3] D. P. Raymer, *Aircraft Design: A Conceptual Approach*, AirLoads.net.
Available: <https://www.airloads.net/Downloads/Textbooks/Aircraft%20Design-A%20Conceptual%20Approach.pdf>. [Accessed: Feb.18,2025].
- [4] Wikipedia contributors, “North American T-6 Texan,” Wikipedia, The Free Encyclopedia.
Available: https://en.wikipedia.org/wiki/North_American_T-6_Texan. [Accessed: Feb.12,2025].
- [5] Wikipedia contributors, “Aeronca Chief Family,” Wikipedia, The Free Encyclopedia.
Available: https://en.wikipedia.org/wiki/Aeronca_Chief_family. [Accessed: Feb.16,2025].
- [6] I. H. Abbott and A. E. von Doenhoff, *Theory of Wing Sections Including a Summary of Airfoil Data*, University of Notre Dame.
Available:
https://www3.nd.edu/~ame40431/AME20211_2021/Other/AbbottDoenhoff_TheoryOfWingSectionsIncludingASummaryOfAirfoilData.pdf. [Accessed: Feb.14,2025].
- [7] XFLR5, *XFLR5 Guidelines v6.10.02*, University of Seville.
Available:
<https://aero.us.es/adesign/Slides/Extra/Aerodynamics/Software/XFLR5/XFLR5%20v6.10.02/Guidelines.pdf>. [Accessed: Feb.11,2025].
- [8] XFLR5, *Point Out of Flight Envelope*, XFLR5 Tech.
Available: http://www.xflr5.tech/docs/Point_Out_Of_Flight_Envelope.pdf. [Accessed: Feb.13,2025].